https://doi.org/10.46813/2024-149-082

CHANGES IN THE STRUCTURE AND PHASE STATE OF ALUMINUM ALLOY 2014, WHICH OCCURRED AS A RESULT OF IRRADIATION WITH AN ELECTRON BEAM

E.M. Prokhorenko[1], V.V. Lytvynenko[1], N.A. Shul'gin[2], I.V. Kolodiy[2], I.G. Tantsyura[2], T.G. Prokhorenko[3]
[1]Institute of Electrophysics and Radiation Technologies NAS of Ukraine, Kharkiv, Ukraine;
[2]National Science Center "Kharkov Institute of Physics and Technology", Kharkiv, Ukraine;
[3]Kharkiv National Automobile and Highway University, Kharkiv, Ukraine
E-mail: forshad58@gmail.com

The use of aluminum alloys in nuclear power is limited by the properties of these alloys in the irradiation zone. The use of electron accelerators is an effective technique for simulating real operating conditions. As a result of irradiation, a whole complex of factors begins to work in the targets, which change the properties of these targets. Pulsed electric and magnetic fields appear, shock waves are generated, and gradient heating occurs. All this together changes the structure and properties of the targets. To irradiate the samples, electron beams with an energy of 8.2...8.3 MeV and a beam current of 0.8 mA were used. The work studied changes in the structural-phase state of an aluminum alloy of type 2014. For samples, before and after irradiation, an analysis of changes in mechanical characteristics (hardness, ultimate strength, proof strength) was carried out. Diffractometric studies were performed. These studies made it possible to determine changes in the phase composition. The intensity values of the diffraction lines were obtained.

PACS: 29.25.Bx, 61.80Fe, 29.27Ac

INTRODUCTION

The use of multicomponent aluminum alloys in industry, automotive, and aircraft manufacturing is due to their wide range of properties. One of the important areas of use of aluminum alloys is energy, including nuclear energy.

Aluminum alloys have high thermal conductivity and electrical conductivity. Alloys have low erosion properties. Aluminum alloys have low weight and have high strength characteristics. The specific strength of aluminum alloys is 2–2.8 times higher than at steel.

Currently, technological standards for the production of aluminum alloys have been developed. Also, methods for producing parts from aluminum alloys are well known and certified. Processing of aluminum alloys is a technologically and relatively cheap process.

However, aluminum alloys have a number of disadvantages. So, during operation, their properties may deteriorate. Strength, electrical and thermal characteristics change

By a perspective method for the change of properties of materials there is irradiation of these materials with ionizing radiation [1–7]. Gamma radiation, X-rays beams, and beams of charged particles (electrons, protons and ions) can be used as ionizing radiation.

Also, the question of influence of ionizing radiation on aluminum alloys is also interesting in scientific plan. Scientific interest is based on the fact that aluminum alloy products are widely used in nuclear energy and exposed to influence of different ionizing radiations.

As a result of irradiation by a beam of accelerated particles, radiation exposure and thermal heating occur. During irradiation, heating has specific characteristics and differs from an ordinary heating. Surface melting is possible.

During irradiation, a change in the phase composition of the sample is possible [5–9]. As a result of irradiation, it is possible the delete of different parasitic phases that contain impurities [8–13]. These processes increase the purity of alloys [7–13]. Also, evaporation of low temperature additives occurs from the surface [6–13].

PURPOSE OF WORK

It is necessary to study how the properties, structural phase state and basic characteristics of aluminum alloy (2014) change as a result of irradiation.

In particular, it is necessary to study the patterns of appearance of various structural disturbances and defects in a sample of alloy of aluminum alloy (2014), which occurred as a result of irradiation with accelerated electron beams. To trace the dynamics of development of structural changes. Determine the general patterns of changes in the structure of alloy of aluminum (2014).

Make a forecast of changes in the physical and mechanical characteristics of the alloy (2014) during irradiation. Based on diffractometric researches, analyze the phase composition of irradiated and non-irradiated samples of alloy. Find out the reasons for changes in the phase composition of samples of alloy.

CONDUCTING EXPERIMENTS AND DISCUSSION OF RESULTS

The work was carried out in several stages. Initially, the material for research was selected. Samples have been prepared for the experiment. Then sources of ionizing radiation and types of ionizing radiation were identified. At the next stage, radiation doses were selected and work on irradiating the samples was performed. Specimens of a certain type are made from

irradiated plates of material. Samples are executed in a kind which is needed for the lead through of mechanical tests and diffractometric researches [8].

The work studied aluminum alloy (2014). An alloy conforms to the requirements which are expounded in normative documents: ISO 209-1 and TU 007-49421776-2011.

The alloy contains the following additives: Al; Cu (3.9…4.8 wt.%), Mg (0.4…0.8 wt.%), Fe (0.7 wt.%), Si (0.6…1.2 wt.%), Zn (0.3 wt.%), Ti (0.1 wt.%), Ni (0.1 wt.%), P (0.03 wt.%), S (0.03 wt.%). The alloy contains manganese (Mn (0.4…1.2 wt.%)). Manganese is a strengthening additive.

Aluminum alloy (2014) has high strength characteristics. Its strength and rigidity is 10 times that of pure aluminum. The alloy has a large anisotropy of mechanical properties. It is used as a building material in nuclear energy and in the construction of storage RAW [14]. Aluminum alloy (2014) is one of the components of composite radiation-protective materials [15–18].

An alloy (2014) was irradiated with accelerated electron beams. The LUE-10 accelerator was used as a source of accelerated electrons. Its main parameters are given in [19]. The electron beam had the following characteristics: electron energy ~ 8.2...8.3 MeV, beam current – 0.8 mA. The condition of vacuum equipment was monitored using IR radiometric methods [20]. To record the temperature of the samples, a remote diagnostic system was used [21]. The remote diagnostic system operates in the optical and infrared range.

The samples were in the form of plates 80×40×3 mm. For different samples, the irradiation time was different. After processing, the samples were kept for 1 year to comply with radiation safety standards. The base (non-irradiated) sample was designated by the index (H). The remaining samples were irradiated over the following time intervals: sample No 4 – 210 s, sample No 6 – 290 s.

During this treatment time, an energy flux density of 10^{15} el./cm^2 was obtained. These fluences are not enough for the evolutionary accumulation of radiation defects. However, in this case, the factor of heating the samples to temperatures of 420…500 °C is triggered. At the same time, recrystallization processes are initiated and secondary phases begin to separate.

Also, in the volume of the sample, the electronic subsystem is activated and a temperature gradient flow appears. The process of electron irradiation enhances these processes. During irradiation, the structure of the surface and the sample itself changes.

The structure of the surface layer of the aluminum alloy was studied using optical microscopes MIM-6, MBS-9, BRESSER-NV-1200. Research was also carried out using a JEOL JSM 840 scanning electron microscope.

The microstructure of the surface of the samples is shown in the photograph (Fig. 1).

The processes of collective recrystallization pass in a sample. Large grains appear. It is visible on the pictures of surface of samples (see Fig. 1).

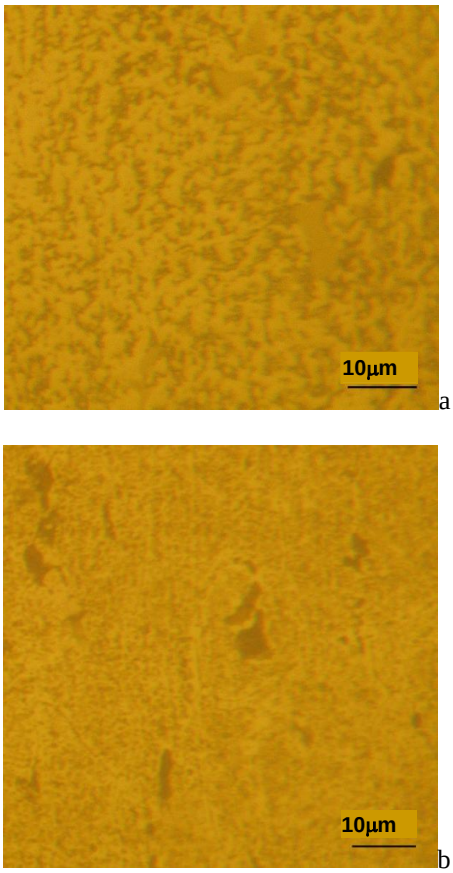

Fig. 1. Surface of samples of alloy 2014: a – sample before irradiation (sample No 3); b – sample after irradiation (sample No 6, exposure 290 s)

Characteristic size of grains of the second phase, makes a few microns (see Fig. 1,a). The amount of grains of the second phase is small. We also observe the appearance of large grains of the third phase. In the original samples, grain boundaries are almost not visible. Presumably, the alloy of primary sample was deformed. There is insignificant metallography texture on a photograph.

The microstructure of the irradiated samples (see Fig. 1,b) differs slightly from the microstructure of the original samples (see Fig. 1,a). In irradiated samples, the metallographic texture is more clearly visible. Grain boundaries and free of excretions near the grains are also visible. All this confirms that recrystallization processes are occurring.

To determine changes in the characteristics of samples of alloy 2014, microhardness measurements were performed. Microhardness was measured both on the surface of the alloy sample and on his depth of the sample. Initially, the microhardness on the surface was measured. The measurements were performed according to the Vickers method.

A LECO LM700AT microhardness tester was used, with an applied load of 25 g. The hardness on the surface was 135.8 kg/mm^2 for the unirradiated sample. The grain size in the original sample (H) turned out to be 29 μm. The grains are unevenly grained. There is a 30% variation in equiaxiality. As a result of irradiation of the sample, its hardness decreased and the grain size increased. Thus, for sample No 6 (irradiation time 290 s), the hardness was 114.1 kg/mm^2, and the grain

size was 38 μm. In the irradiated sample, the microhardness decreased and the grain size increased.

All these changes occur as a result of collective recrystallization processes, which are initiated by the action of an accelerated electron beam. Large grains appear on the surface, which are surrounded by smaller grains (see Fig. 1,b).

In order to obtain macromechanical characteristics, tests were performed on a tensile testing machine. For this purpose, samples of a certain shape were made from alloy plates, which are used in a tensile testing machine (length 35 mm, width 2 mm and thickness 4 mm). Tests were carried out at a temperature of 300 K. Photographs of the surface of the ruptures and their locations are presented in [8].

It was found from experiments that the break point is in the middle of the sample. The location of break does not depend on the radiation dose. The breaks were fragile. All samples have a slight narrowing of neck of break. For all samples, there is no elongation of neck of break. The diagrams of stretch are shown on the graphic in Fig. 2.

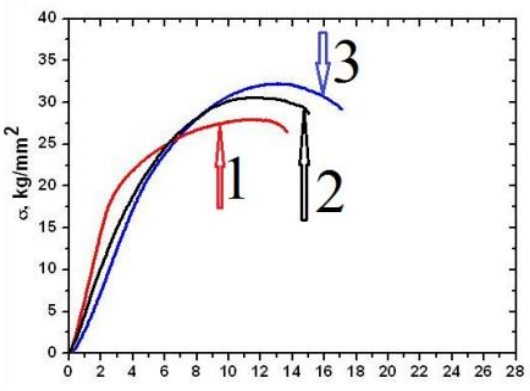

Fig. 2. Graphs of stretch diagrams:
1 – unirradiated sample (No H);
2 – irradiation 4 (210 s); 3 – irradiation 6 (290 s)

From the graphs we find that the force that was applied to the non-irradiated sample is higher than the forces that were applied to the irradiated samples. That is, at the initial stages of deformation, softening processes occur in irradiated samples, which are greater than in non-irradiated samples. With further stretching (deformation), the opposite effect occurs. That is, there is a slight strengthening of irradiated samples compared to non-irradiated samples.

Also, the following parameters were measured: tensile strength (σ_B), yield strength (σ_{02}), maximum elongation to failure (Table 1).

From a Table 1 evidently, that these sizes are increased, when the time of exposure to the electron beam increases of the sample of alloy.

The analysis of presence and distributing of including of different phases was conducted in material of alloy 2014.

Manganese is present in the alloy in the form of dispersed particles ($Al_{12}Mn_2Cu$) (phase of T). Inclusions based on manganese (Mn_3Al_2) were also discovered [4, 7–13, 22]. The phases of manganese ($Al_{12}Mn_2Cu$ and Mn_3Al_2) improve the mechanical properties of alloy 2014.

Table 1

Experimental values of σ_B, σ_{02}, maximum elongation to break

Sample Number (exposure time, s)	Tensile strength σ_B, kg/mm^2	Yield Stress σ_{02}, kg/mm^2	Maximum elongation to break, %
H	28	20	14
4 (210)	30	23	15
6 (290)	33	27	17

It has been found that silicon forms the phases of Mg_2Si and $W(Al_xMg_5Cu_6Si_4)$ [4, 7–13, 22]. At the same time, the main phases that contribute to hardening are reduced.

In addition, alloy 2014 contains inclusions of impurities that worsen the mechanical characteristics. Among them are inclusions of iron, sulfur, and phosphorus [8–13, 22].

Iron is found in the form of impurities. Basically, these are insoluble inclusions in the form of plates, which have the following composition $(MnFe)Al_6$. In addition, an alloy of Al_2Cu_2Fe is formed [4, 7–13, 22]. This alloy does not dissolve in aluminum.

These inclusions also bind copper. The presence inclusions of iron ($(MnFe)Al_6$ and Al_2Cu_2Fe) in the alloy of 2014 reduces the strength and ductility. Therefore, in the alloy 2014, the amount of impurities of iron should not exceed 0.7% [8–13].

Alloy 2014 contains phosphorus and sulfur. The amount of sulfur and phosphorus impurities is small. However, even small quantity of phosphorus and sulfur impurities worsen the characteristics of alloy 2014 alloy and reduce its strength characteristics [8].

We studied how the amount of inclusions of sulfur and phosphorus changed as a result of irradiation. After irradiation of sample 2014, the amount of phosphorus and sulfur inclusions decreased. Their number is minimal for the sample of alloy with the maximum time of irradiation. Consequently, as a result of processing the samples of alloy with an electron beam, the material is cleaned.

X-ray diffraction analysis of the samples showed that there is a change of phases in an alloy as a result of irradiation with an accelerated electron beam. A decrease in the inclusions of Mn_3Al_2 and Mg_2Si was found. These inclusions increase the hardness of alloy 2014. Their reduction reduces the characteristics hardness. Measurements hardness at the surface and in the cross section confirmed that the decrease in the alloy of inclusions of Mn_3Al_2 and Mg_2Si contributed to the decrease in the hardness of alloy 2014.

Measurements of microhardness in the cross section of the sample were performed. For this, samples were cut from the plates irradiated and cross sections were made. A microhardness tester PMT-3 was used as a measuring device, with a load of 50 g.

The results are the average hardness values obtained from ten measurements. Measurements were made for the front plane of the sample (1) and in the middle of the sample (2). The results are shown in Table 2.

Table 2

Experimental values of microhardness on surface of sample (1), in the middle of sample (2)

Sample Number (time, s)	Microhardness (1), kg/mm^2	Microhardness (2), kg/mm^2
H (0)	129.7	124.2
6 (290)	84.5	89.2

From the Table 2 evidently, that in the initial sample, the microhardness near the surface is slightly higher than in the middle of the plate. The reason may be the hardening of the surface layers due to the inhomogeneity of the deformation during rolling. After irradiation, we observe a decrease in microhardness on 50%.

The decrease in microhardness after irradiation is apparently associated with thermal effects during irradiation. Recrystallization processes also have a significant effect on microhardness. It was also found that after irradiation, the microhardness of the middle of the sample is greater than the microhardness of the surface layer on the side of irradiation.

The reason that the microhardness in the central part of sample is higher than on the surface may be the appearance of the "pre-decomposition" process. That is, along with the recrystallization processes for the main phase, which lead to a decrease in microhardness, a "pre-decomposition" process appears for the second phase.

As a result of this process, the second phase is formed and its volume fraction increases. These effects occur as a result of the appearance and growth of particles of the second and even third phase. These processes lead to increase microhardness in the central part of the sample. The appearance of particles of the second phase was noted on the diffraction patterns Fig. 3.

To perform diffractometric studies, an X-ray diffractometer (DRON-4-7) was used. X-ray diffractometer operates in copper Cu-Kα radiation. When working on it, a nickel absorbing filter is used. This filter has selective absorptive properties. The resulting diffracted radiation was recorded using a scintillation detector.

The diffraction patterns were processed using standard procedures: a) delete of background image; b) performing of procedure of smoothing; c) selection of size of peak of $K\alpha_1$-dubleta; d) approximation of the diffraction peak using the pseudo-Voigt function.

Carrying out these procedures makes it possible to determine the characteristics of diffraction maximums. Among the characteristics of diffraction maximums, the most informative are: angular position 2θ, intensity I, half-width FWHM, integral width B.

Samples were prepared for measurements. The samples had dimensions of 18×18×4 mm. After the leadthrough of measurings were got diffraction patterns (see Fig. 3).

On Fig. 3.a shows a graph of the diffraction pattern of the original sample, this was designated by the index (H). Lattice parameter a = 4.0504 Å. With this sensitivity of the method, no traces of other phases were detected. The intensity distribution for lines of aluminum differs from the textureless state. The surface texture is complex for the unirradiated sample 2014. The reason for the appearance of a complex texture may possibly be the rolling of samples during the manufacturing process.

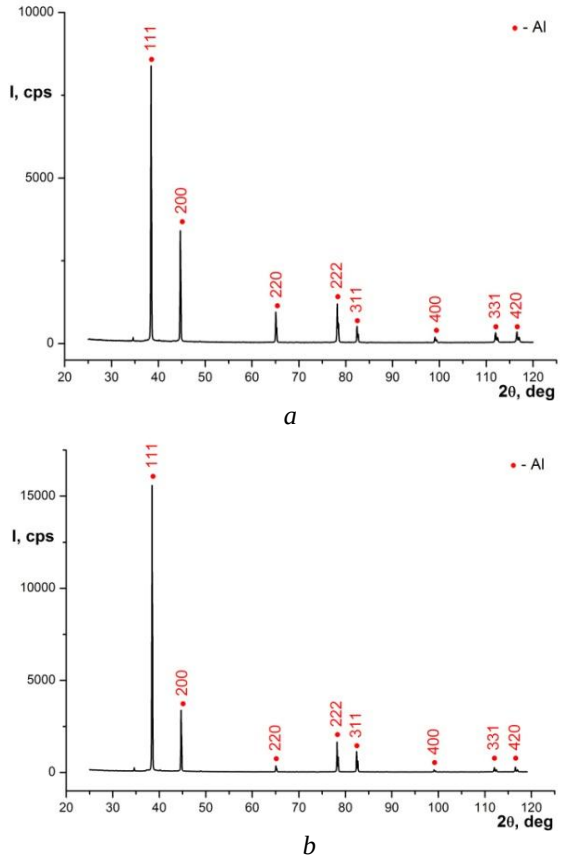

Fig. 3. Diffraction patterns of the surface of alloy 2014: a – unirradiated sample (No H); b – irradiated sample No 6 (surface from the irradiation side, exposure 290 s)

At the next stage, the diffraction pattern was studied, which is presented in Fig. 3,b. This diffraction pattern was obtained during the study of the irradiated surface of sample No6. The parameter of grate of alloy 2014 was found, which had the value a = 4.0499 Å. We have an insignificant difference of parameters of grate of the irradiated and non-irradiated alloy samples. The intensity distribution of lines of aluminum for the irradiated sample also differs from that of the sample with a textureless surface structure.

It should be noted that we have one very significant limitation. It concerns the depth of penetration of radiation into the sample during its examination. The depth of penetration of radiation of X-ray into the material of sample (depth of the information layer) is not a constant value. The penetration depth into the sample depends on two parameters. One of these parameters is a type of material and its component composition.

Another very important parameter is the value of the diffraction angle 2θ. Moreover, there is a directly proportional relationship. That is, the smaller the angle 2θ, the smaller the information layer. For alloy 2014, the maximum penetration depth is 53 μm, at for angle of 2θ = 180°. These values are given for Cu-Kα radiation.

X-ray diffraction analysis of the samples showed that as a result of irradiation with an accelerated electron beam, a phase change occurs in the alloy. A decrease in Mn_3Al_2 and Mg_2Si inclusions was detected. These inclusions increase the hardness of alloy 2014. Their reduction reduces the hardness characteristics. Hardness measurements on the surface and in the cross section confirmed that the decrease in the Mn_3Al_2 and Mg_2Si inclusions in the alloy contributed to the decrease in the hardness of alloy 2014.

We also investigated how, as a result of irradiation, the amount of including of sulfur and phosphorus changed. After irradiation of sample 2014, the amount of phosphorus and sulfur inclusions decreased [8–13]. Their amount is minimal for the alloy sample with the maximum irradiation time. Consequently, as a result of processing of samples of alloy with an electron beam, the material is cleaned.

When analyzing the diffraction patterns in Fig. 3 we observe that the intensity of lines of aluminum for the irradiated alloy sample is greater than for the non-irradiated alloy sample. Apparently, this is due to the increase of purity of aluminum alloy.

For research, the characteristic parameters of diffraction lines were calculated. With their help, it becomes possible to find the change in the characteristics of sample of 2014. The values of these parameters are given in Tables 3 and 4.

Table 3

Parameters of the diffraction lines of the non-irradiated sample of alloy 2014 (No H)

hkl	2θ, deg	I, cps	FWHM, deg	Int.width B, deg
111	38.418	7290.9	0.1279	0.1511
200	44.669	3160.8	0.1276	0.1546
220	65.052	884.9	0.1400	0.1735
311	78.186	1177.7	0.1535	0.1913
222	82.392	483.8	0.1564	0.1890
400	99.040	165.8	0.2042	0.2687
331	111.982	287.3	0.2224	0.3035
420	116.535	303.4	0.2449	0.3230

Table 4

Parameters of diffraction lines of the irradiated sample of alloy 2014 (No 6)

hkl	2θ, deg	I, cps	FWHM, deg	Int.width B, deg
111	38.435	13975.7	0.1102	0.1339
200	44.676	3334.5	0.1094	0.1364
220	65.045	330.6	0.1476	0.1797
311	78.209	1620.2	0.1235	0.1490
222	82.411	1137.0	0.1295	0.1565
400	99.057	131.4	0.1439	0.2149
331	112.020	238.9	0.1699	0.2399
420	116.550	261.9	0.1647	0.2369

Analysis of diffraction lines showed that as a result of irradiation, the width of the radiation characteristics decreases. We observe a decrease in the integral width (B) for irradiated samples. Also, the half-width of FWHM lines after irradiation decreased significantly compared to the initial state (see Tables 3, 4 and Fig. 4).

When analyzing the data presented in the graphs (see Fig. 4), one interesting anomaly was discovered. We observe differences in the integral width and width (FWHM) values for line 220. The integral width (I B) and width (FWHM) values for the irradiated sample are higher than for the unirradiated sample. There is no reliable explanation for this effect yet. The reason may be the orientation of the crystallites of the second phase, which were formed as a result of irradiation.

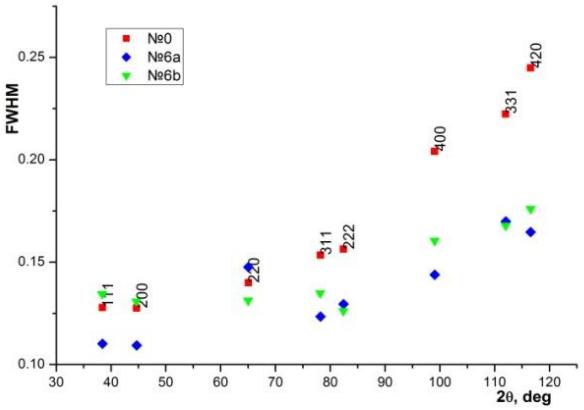

Fig. 4. Dependence of the half-width of the FWHM parameter on the angle of diffraction (2θ). Marker red square – sample without irradiation. Marker blue rhombus – sample after irradiation (No 6, irradiation time – 290 s)

Base samples and irradiated of samples of alloy 2014 were heterophase. The appearance of a heterophase structure is due to the fact that the alloy material is heated, pre-melting processes and deposition of the material onto a colder substrate are possible. The substrate is the bottom layer of material of alloy, which does not have time to warm up.

Note that the dimensions, quantity, and shape of the phases determine the properties of the aluminum alloy samples. The physical properties of heterophase bodies are not an additive sum of the properties of the phases of the body, since there are additional interphase boundaries and additional internal stress fields appear that arise when different phases come into contact [23].

The position and distribution of aluminum phases have a significant influence on the characteristics of the alloy. Important parameters that change the characteristics of heterophase alloys are the characteristics of the distribution and mutual location of interphase boundaries. It is also necessary to take into account the presence of different internal defects [23].

When samples are irradiated, phase transformations occur. In the initial phase, separate areas or separate crystals of the second and third phases appear. These phases are more steady thermodynamically.

Consequently, irradiation with a beam of accelerated electrons affects the processes of structural phase transformations.

Irradiation is accompanied by the appearance of zones with increased values of pressure and temperature around the electron tracks [24]. In turn, overheated regions can form a local liquid phase, which causes an

increase in volume and the generation of expansion-compression waves [25, 26]. It should also be taken into account the presence of an aluminum oxide film on the surface, the processes of which can also be reflected in the nature of structural-phase transformations at the interface with a non-oxidized alloy, as is typical for zirconium oxide, for example [27]. Accordingly, in the sample of alloy that is irradiated, we obtain various heterophase structures. Processing samples using accelerated electron beams makes it possible to control the processes of formation of a heterophase structure and impart the necessary properties to the material of sample. The proposed type of material processing may be promising not only for modifying mechanical properties, but also as a method of radiation-thermal annealing of materials and products operated under conditions of long-term vacuum irradiation and having increased requirements for residual gas evolution [28].

CONCLUSIONS

1. The intensity of diffraction lines for irradiated samples is higher than for non-irradiated samples. This is due to the cleaning of the alloy surface from inclusions of impurities of phosphorus and sulphur.

2. It was found that, after the irradiation of samples of alloy of type 2014, the parameter of grate decreased.

3. There is growth of grains of aluminium at an irradiation. The hardness of the samples decreases.

4. A change in the phase composition of the alloy was detected. Grains of the second phase and separate grains of the third phase appear.

5. As a result of irradiation, increases the half-width of diffraction lines (integral width and FWHM width).

6. It was found that, as a result of irradiation, the half-width of line 220 did not change. This is anomalous.

REFERENCES

1. Lu Diankun, Gao Bo, et al. High-Current Pulsed Electron Treatment of Hypoeutectic Al-10Si alloy // *High Temp. Mater. Proc.* 2017, N 36(1), p. 97-100.

2. A. Weisenburger, W. An, et al. Intense Pulsed Electron Beams Application of Modified Materials // *Acta Physica Polonica* A. 2009, v. 115, N 6, p. 1053-1055.

3. O.V. Manuilenko, E.M. Prokhorenko, K.V. Pavlii, B.V. Zajtsev, S.N. Dubniuk, V.V. Lytvynenko, T.G. Prokhorenko. Changes of the radiation characteristics of surface of tungsten as a result of influence of helium ion beams // *Problems of Atomic Science and Technology (PAST).* 2022, N 3(139), p. 36-41; https://doi.org/10.46813/2022-139-036

4. V.V. Bryukhovetskiy, N.I. Bazaleev, V.F. Klepikov, V.V. Litvinenko, O.E. Bryukhovetskay, E.M. Prokhorenko, V.T. Uvarov, A.G. Ponomar'ov. Features of gelation of surface of industrial aluminium alloy 6111 in the area of influence of impulsive bunch of electrons in the mode of premelting // *PAST*. 2011, N 2(72), p. 28-32.

5. V. Tarelnyk, V. Martsynkovskyy, et al. New method for strengthening surfaces of heat treated steel parts // *IOP Conference Series: Materials Science and Engineering.* 2017, v. 233, N 1, art. no. 012048.

6. J. Cai et al. Deformation mechanism and microstructures on polycrystalline aluminum induced by high-current pulsed electron beam // *Chinese Science Bulletin*. 2013. v. 58, issue 20, p. 2507-2511.

7. V.V. Bryukhovetsky et al. The features of the structural state and phase composition of the surface layer of aluminum alloy Al-Mg-Cu-Zn-Zr irradiated by the high current electron beam // *Nuclear Inst. and Methods in Physics Research B*. 2021, v. 499, p. 25-31; https://doi.org/10.1016/j.nimb.2021.02.011

8. E.M. Prokhorenko, V.V. Lytvynenko, V.V. Bryukhovetskiy, N.A. Shul'gin, I.V. Kolodiy, I.G. Tantsyura, T.G. Prokhorenko. Modification of the structurally the phase state of aluminum alloy as a result of radiation thermal treatment // *PAST.* 2022, N 1(137), p. 122-129; https://doi.org/10.46813/2022-137-122

9. E.M. Prokhorenko, V.F. Klepiakov, V.V. Lytvynenko, P.A. Khaymovich, N.A. Shul'gin, A.I. Morozov. Diagnostics of processes of wear of materials of balls drum mills // *Eastern European Journal of Enterprise Technologies*. 2015, N 1/5(73), p. 14-20.

10. Shang Li, Xuanpu Dong, et al. Status and Perspective of High-Energy Beam Surface Strengthening: High-Speed Steel // *Materials.* 2022, N 15(17), p. 6129; https://doi.org/10.3390/ma15176129

11. E.M. Prokhorenko, V.V. Lytvynenko, O.A. Melyakova, Yu.F. Lonin, A.G. Ponomarev, V.T. Uvarov, N.A. Shul'gin, T.G. Prokhorenko, R.I. Starovoytov, A.I. Morozov, S.R. Artemev. Strengthening of the surface of steel (9KhFM) exposed to a high-current electron beam // *PAST.* 2020, N 1(125), p. 167-172.

12. E.M. Prokhorenko, V.V. Lytvynenko, O.A. Melyakova, Yu.F. Lonin, A.G. Ponomarev, V.T. Uvarov, N.A. Shul'gin, T.G. Prokhorenko. Modification of structure of the surface of steel (KhGS) as result of influences of high-current electron beem // *PAST.* 2020, N 2(126), p. 47- 53.

13. Y. Qin, C. Dong, Z. Song, et al. Deep modification of materials by thermal stress wave generated by irradiation of highcurrent pulsed electron beams // *Journal of Vacuum Science and Technology A*. 2009, v. 27, N 3, p. 430-435.

14. V.F. Klepikov, E.M. Prokhorenko, V.V. Lytvynenko, S.E. Donets, V.N. Robuk, T.G. Prokhorenko, V.T. Uvarov, A.G. Ponomarev, Yu.F. Lonin The use of high-current relativistic electron beams for the study of the effects of ionizing radiation on materials storage RAW // *PAST*. 2016, N 2(102), p. 72-77.

15. V.F. Klepikov, E.M. Prokhorenko, V.V. Lytvynenko, A.A. Zaharchenko, M.A. Hazhmuradov. Control of macroscopic characteristics of composite materials for radiation protection // *PAST.* 2015, N 2(96), p. 193-196.

16. V.F. Klepikov, E.M. Prokhorenko, V.V. Lytvynenko, A.A. Zaharchenko, M.A. Hazhmuradov. Perfo-rmance ratio hardness characteristics polystyrene-metal composite materials // *PAST.* 2015, N 5(99), p. 36-42.

17. E.M. Prokhorenko, V.V. Lytvynenko, A.A. Zaharchenko, M.A. Hazhmuradov, T.G. Prokhorenko. Studying the changes in the characteristics of radiation-protective composition materials in dependence on homogeneity of distributing of metal components // *PAST*. 2019, N 2(120), p. 121-126.

18. V.F. Klepikov, E.M. Prokhorenko, V.V. Lytvynenko, A.A. Zaharchenko, M.A. Hazhmuradov. Application of methods of mathematical modeling for determining of radiation-protective characteristics of polystyrene-metal composite materials // *PAST*. 2016, N 3(103), p. 123-127.

19. N.I. Ayzatsky, V.N. Boriskin, et al. Radiation technology with the use of electron and bremsstrahlung. // *PAST*. 1999, N 1(33), p. 61-63.

20. E.M. Prokhorenko, V.F. Klepikov, V.V. Lytvynenko, N.I. Bazaleyev, I.I. Magda, T.G. Prokhorenko, A.I. Morozov. Application of ir-radiometric diagnostics for control of vacuum connections of electrophysical installations // *PAST*. 2018, N 1(113), p. 212-217.

21. V.N. Boriskin, S.K. Romanovsky, et al. Optical monitoring the temherature of ojects irradiated at an electron accelerator // *PAST*. 2015, N 6(100), p. 105-107.

22. Dzh. Fellouz. *Fraktography and Atlas of fraktographs.* Ohio: "Metals park", 1982, 489 p.

23. Yi. Guo, Ch. Paramatmuni, et al. Void Nucleation and Growth from Heterophases and the Exploitation of New Toughening Mechanisms in Metals // *Crystals*. 2023, v. 13(6), p. 860; https://doi.org/10.3390/cryst13060860.

24. A.Yu. Didyk et al. Change in sample surface area during formation of cylindrical tracks as a result of high-energy heavy-ion irradiation. // *Metallofizika i Noveishie Tekhnologii*. 2010, v. 32(3), p. 357-363 (in Russian).

25. V.P. Poida et al. Structural changes during superplastic deformation of high strength alloy 1933 of the Al-Mg-Zn-Cu-Zr system // *Physics of Metals and Metallography*. 2013, v. 114, N 9, p. 779-788.

26. V.V. Bryukhovetskij et al. Effect of the pulsed electron irradiation on superplasticity properties of duraluminum. // *Fizika i Khimiya Obrabotki Materialov*. 2002, N 4, p. 33–38 (in Russian).

27. V.I. Slisenko et al. The dynamics of crystal lattice of solid solution based on zirconium dioxide // *Journal of Physical Studies*. 2021, N 25(4), p. 4601-1–4601-6.

28. P. Gladkikh et al. Injection system for Kharkov X-ray source nestor // *EPAC 2006 – Contributions to the Proceedings*, 2006, p. 2038-2040.

Article received 25.07.2023

ЗМІНИ СТРУКТУРИ ТА ФАЗОВОГО СТАНУ АЛЮМІНІЄВОГО СПЛАВУ 2014, ЯКІ НАСТУПИЛИ У РЕЗУЛЬТАТІ ОПРОМІНЕННЯ ПУЧКОМ ЕЛЕКТРОНІВ

Є.М. Прохоренко, В.В. Литвиненко, М.А. Шульгін, І.В. Колодій, І.Г. Танцюра, Т.Г. Прохоренко

Використання алюмінієвих сплавів у атомній енергетиці обмежується властивостями цих сплавів у зоні опромінення. Застосування прискорювачів електронів є ефективною методикою для моделювання реальних умов експлуатації. У результаті опромінення у мішенях розпочинає працювати цілий комплекс факторів, які змінюють властивості цих мішеней. З'являються імпульсні електричні та магнітні поля, відбувається генерація ударних хвиль, здійснюється градієнтне нагрівання. Все це в комплексі змінює структуру та властивості мішеней. Для опромінення зразків застосовували пучки електронів з енергією 8,2…8,3 МеВ та струмом пучка 0,8 мА. У роботі вивчалися зміни структурно-фазового стану алюмінієвого сплаву типу 2014. Для зразків до та після опромінення проводився аналіз змін механічних характеристик (твердості, граничної міцності, умовної межи плинності). Виконано дифрактометричні дослідження, які дозволили визначити зміни фазового складу. Отримано значення інтенсивності дифракційних ліній.